Improvements in PIXE analysis of hourly particulate matter samples

G. Calzolai [a,b,*], F. Lucarelli [a,b], M. Chiari [b], S. Nava [b], M. Giannoni [b,c], L. Carraresi [a,b], P. Prati [d], R. Vecchi [e]

[a] Department of Physics and Astronomy, University of Florence, Via G. Sansone 1, 50019 Sesto Fiorentino (Fi), Italy
[b] National Institute of Nuclear Physics (INFN), Division of Florence, Via G. Sansone 1, 50019 Sesto Fiorentino (Fi), Italy
[c] Department of Chemistry, University of Florence, Via della Lastruccia 3, 50019 Sesto Fiorentino (Fi), Italy
[d] Department of Physics, University of Genoa and INFN Division of Genoa, Via Dodecaneso 33, 16146 Genoa, Italy
[e] Department of Physics, Università degli Studi di Milano and INFN Division of Milan, Via Celoria 16, 20133 Milan, Italy

ABSTRACT

Most air quality studies on particulate matter (PM) are based on 24-h averaged data; however, many PM emissions as well as their atmospheric dilution processes change within a few hours. Samplings of PM with 1-h resolution can be performed by the streaker sampler (PIXE International Corporation), which is designed to separate the fine (aerodynamic diameter less than 2.5 μm) and the coarse (aerodynamic diameter between 2.5 and 10 μm) fractions of PM. These samples are efficiently analyzed by Particle Induced X-ray Emission (PIXE) at the LABEC laboratory of INFN in Florence (Italy), equipped with a 3 MV Tandetron accelerator, thanks to an optimized external-beam set-up, a convenient choice of the beam energy and suitable collecting substrates. A detailed description of the adopted set-up and results from a methodological study on the detection limits for the selection of the optimal beam energy are shown; the outcomes of the research on alternative collecting substrates, which produce a lower background during the measurements, and with lower contaminations, are also discussed.

1. Introduction

Atmospheric aerosols (also called *particulate matter*, PM) have been recognized as relevant factors for both human health and environmental issues, and this has led to important efforts from both a scientific and a political point of view to develop effective policies for the aerosol pollution abatement. More in detail, several studies have connected human aerosol exposure with serious illnesses [1], pointing to the potential of smaller particles to get deeper into the respiratory system and eventually into the blood circulation system, possibly carrying harmful compounds or elements they are composed of. As concerns the effects on the environment, beyond reduction of the visibility and acidic rains, atmospheric aerosols have been recognized as influencing the Earth climate at a global level, via both direct and indirect effects primarily affecting the global radiation budget and the hydrological cycle; nevertheless, due to the complex feedbacks in climate phenomena, the quantification of the effects of aerosol is still subject to large uncertainties [2]. Several properties of aerosol, such as chemical composition and aerosol particle dimensions, contribute to determine the aforementioned effects. Concerning particle

dimensions, aerosols are conveniently classified on the basis of their aerodynamic diameter (d_{ae}), defined as the diameter of a sphere of unit density with the same aerodynamic characteristics as the considered particle [3]; aerosol with particles with $d_{ae} < 10$ μm are called PM_{10}, while $PM_{2.5}$ includes only particles with $d_{ae} < 2.5$ μm.

Atmospheric aerosols may have several sources, both natural (e.g., sea-spray, mineral dust) and anthropogenic (e.g., traffic, industry, combustions). Despite transport and dilution processes, aerosols maintain the characteristic elemental ratios of the emitting sources, which may be therefore determined. Nevertheless, only a few compounds are univocal markers of a single source (e.g., levoglucosan for biomass burning, radiocarbon for fossil/modern sources [4]); therefore, source apportionment studies are usually performed by means of statistical multivariate analysis, needing as input several data of aerosol mass concentration and composition as measured at the receptor (sampling) site. The most widely used model for source apportionment, nowadays, is the Positive Matrix Factorization analysis [5].

1.1. High time resolution samplings

Many PM emission processes change within a few hours, as well as the atmospheric transport and dilution processes, which are influenced by the rapid changes of several meteorological

* Corresponding author at: Via G. Sansone 1, I-50019 Sesto Fiorentino (Firenze), Italy. Tel.: +39 055 4572727.
  E-mail address: calzolai@fi.infn.it (G. Calzolai).

parameters (e.g., wind intensity and direction, precipitation) and the strong diurnal pattern of the boundary level evolution. Consequently, both aerosol concentration and composition may significantly change on the 1-h scale; nevertheless, most air quality studies in urban areas, as well as several monitoring campaigns in remote areas, are based on 24-h averaged data, and are therefore unable to track the rapid changes of the impact of the different sources. Samplings performed with high time resolution, that is with a 1-h (or less) timescale, give a better insight on aerosol emission, transport, dilution and deposition processes, as well as they give a better quantification of the human exposure to pollutants, making it possible to assess severe (even if time-limited) episodes [6–9]. Furthermore, high time resolution data enhance the potential of source apportionment due to the fact that receptor models benefit from high inter-sample variability in the source contributions and that information on the time pattern of the contributions of a source may help in identifying it [10–15]. However, the analysis of samples collected with high-time resolution requires a significant effort from an analytical point of view, since, as an example, one week of sampling with 1-h resolution results in 168 samples.

1.2. PIXE measurements

Measurements with Particle Induced X-ray Emission (PIXE) have been used for the analysis of aerosol samples since the birth of this technique; nevertheless, nowadays PIXE has to cope with several competitive techniques that have improved over the years, such as Inductively Coupled Plasma Mass Spectrometry (ICP-MS), Inductively Coupled Plasma Atomic Emission Spectroscopy (ICP-AES), Energy Dispersive X-ray Fluorescence (ED-XRF) and Synchrotron Radiation XRF (SR-XRF) [16]. However, PIXE still has an important role due to its main features, such as high measuring speed, high sensitivity, measures on the sample as-is (without any pre-treatments) and the capability of detecting all the soil-related elements. In particular, these characteristics make PIXE the ideal technique for the analysis of high-time resolution samples, as they are characterized by low mass deposits and a high number of collected samples in a campaign. At the LABEC laboratory of Florence an external beam line is fully dedicated to the analysis of aerosol samples, and has been widely used for the analysis of samples collected with 1-h resolution using the streaker sampler. Although a recent feasibility study demonstrated that a specialized custom-made ED-XRF system may represent a promising solution for elemental analysis of streaker samples, even for low-Z elements, PIXE still remains unrivalled as regards sensitivity and measurement throughput [17].

In this paper, after giving a description of the sampling with the streaker device, we address the improvements that have been made to the LABEC experimental set-up to fully exploit the capabilities of PIXE for the analysis of the streaker samples; furthermore, we report the results on the choice of optimal measurement parameters and substrates suitable for both sampling and subsequent analysis.

2. The streaker sampler

For the sampling with hourly resolution, the streaker sampler of PIXE International Corporation has been adopted [18]. In such sampler, the airflow is subject to abrupt direction changes in order to select different particle dimensional classes. More in detail, particles with $d_{ae} > 10\ \mu m$ impact on a pre-impactor inhibiting their deposition on the collection substrates; particles with a smaller diameter (PM_{10}) follow the air-stream inside the sampler, where a new abrupt direction change allows the separation of PM_{10} into

coarse and fine fractions: in fact, coarse particles, i.e., particles with d_{ae} in the range 2.5–10 μm, impact on an impaction foil and are so collected for subsequent analysis; fine particles, i.e., with $d_{ae} < 2.5\ \mu m$, follow the air flow and are collected on the following stage, by means of a filtration foil. The impaction and filtration foils are paired in a cartridge, which can rotate either with a constant speed or with discrete steps. Thanks to the rotation, particles are collected on the two substrates in continuous deposits (the "streak") when a constant rotation speed is used, or as a series of discrete spots on a circumference otherwise. In most of the applications, the rotation speed is set to a constant value allowing the sampling for 168 h, i.e., one week, on the two collection foils. The dimensions of the sucking orifice (which determine the spot dimension on the filtration foil) may be changed by choosing the most suitable nozzle from a set of given ones; to avoid filter clogging, we usually use the 2 mm wide orifice.

The sampler needs a 1 l/min air flow in order to ensure the correct separation of particles depending on their dimensions, i.e., to ensure the desired cut diameters for both the pre-impaction and impaction stages. Therefore, for the control of the streaker sampler a modified Echo-PM unit by TCR-Tecora is used: this unit provides a pumping system allowing a stable 1 l/min flow, the alimentation for the streaker stepper motor, and an easily accessible software for sampling programming. The control unit also stops the sampling if the set flow is not attained (e.g., incorrect cartridge mounting, clogging of the filtration foil...). Furthermore, the use of a data logger by GRIFO enables the record of all sampling data, thus allowing the a posteriori check of the sampling performance, and temperature and pressure data every 5 s.

As collecting substrates, PIXE International provides Nuclepore filters ($C_{15}H_{14}CO_3$, 10 μm thick) for the filtration stage and Kapton foils ($C_{22}H_{10}N_2O_4$, 7.5 μm thick) for the impaction stage; the latter ones are coated in order to prevent the bouncing of particles.

3. Methods

3.1. Optimized PIXE experimental set-up

In order to fully exploit the potential of PIXE in the analysis of the aerosol samples, an external beam line fully dedicated to this application has been developed at the LABEC laboratory of INFN in Florence, equipped with a 3 MV Tandetron accelerator; such set-up has been constantly improved taking advantage of the technological advancements in terms of X-ray detectors. Since its first installation in 2003, the set-up has been based on a two-detector system [19], optimized for the detection of low-Z and medium-high-Z elements, in order to take into account the differences in the X-ray production cross sections, spanning over several orders of magnitude. In its first version, such set-up included two Si(Li) detectors, one characterized by a thin entrance window and a small active area, the other by large active thickness and area, to effectively detect both low-energy and medium-high energy X-rays, that is low-Z and medium-high-Z elements, respectively (an extensive description of this set-up may be found in [20]). With the advent and the unceasing development of Silicon Drift Detectors (SDDs), leading to devices with larger and thicker active areas, Si(Li) detectors have been dismissed as their performances have been more and more superseded by those of SDDs; in fact, SDD provide better resolution with modest cooling (down to −40 °C) achievable with Peltier cells and can cope with higher counting rates (up to 50 kHz at 0.5 μs shaping time). Due to these features, first the Si(Li) detector dedicated to low-Z elements was replaced by a 10 mm^2, 280 μm thick SDD [21], then, when thicker crystals became available, also the Si(Li) for medium-high-Z elements was replaced by a SDD, having a 80 mm^2 active area and a

450 μm thickness [22]. Recently, the set-up has been further improved with the upgrade of the SDD dedicated to the low-Z elements, and the introduction of a second SDD for medium-high-Z elements, as shown in Fig. 1. All the SDDs in our system were supplied by Ketek GmbH.

More in detail, the proton beam is extracted in air through a 500 nm Si_3N_4 window and the samples are positioned at about 1 cm distance from it, perpendicularly to the beam. A collimator at the end of the beam line sets the beam spot to 1×2 mm^2; the charge flown during the measurement is simply measured by integrating the beam current on a graphite Faraday cup positioned just behind the samples. Movement of the samples on the x–y axes (perpendicular to beam direction) and change of the samples by rotation of the sample holder (or the streaker foil) are both remotely controlled by the acquisition system.

As concerns the SDD dedicated to low-Z elements, in the previous set-up a 10 mm^2 (collimated to 7 mm^2), 280 μm thick SDD was used. As in the previous set-ups, the use of a thin (8 μm) Be window and the saturation of the volume between the entrance window and the target with helium enabled the detection of X-rays down to around 1 keV, i.e., the detection of elements down to Na (Z = 11). The SDD was positioned at about 145° with respect to the beam direction, at about 6 cm distance from the target; a magnetic proton deflector was installed to prevent the damage to the detector by backscattered protons, designed to deflect protons up to 6 MeV in energy. In the newly upgraded set-up, this SDD has been replaced by a 40 mm^2 (collimated to 30 mm^2 by a Ta–Cr–Ti–Al multilayer collimator, to shield the outer part of the area, where incomplete charge collection may happen [23]), 450 μm thick SDD, having 140 eV FWHM energy resolution at the 5.9 keV Mn Kα line and 1 μs shaping time. The position of the detector has been maintained, although the distance of the new SDD from the target has been necessarily increased to about 9 cm due to the larger length of the new magnetic proton deflector. In fact, keeping the previous magnetic field (0.5 T), the length of the magnets had to be increased in order to shield the larger crystal by backscattered protons up to 4 MeV (indeed higher energy protons are not suited for PIXE analysis of aerosols, as will be discussed later in Section 3.2). In the upgraded set-up the saturation with helium is no longer limited to the volume between the entrance
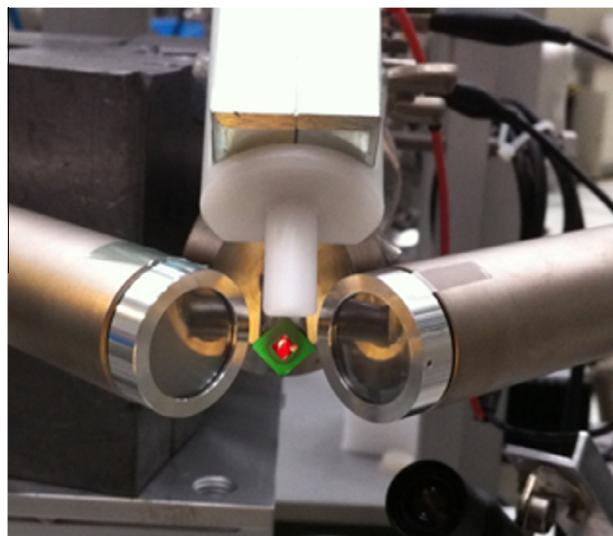
window and the target, but it has been implemented also in the volume between the target and the Faraday cup. In Fig. 2 a comparison of spectra acquired with and without the helium flow behind the sample is shown. The quantification of potassium by its Kα line highly beneficiates by the reduction of the signal from the argon in the residual air behind the target.

As concerns the detection of the medium-high Z elements, in the previous set-up a KETEK SDD was introduced, with the following characteristics: 113 mm^2 area (collimated to 80 mm^2 by a Ta–Cr–Ti–Al multilayer collimator, again to shield the detector outer area where an incomplete charge collection may take place), 450 μm thickness, 165 eV FWHM energy resolution at the 5.9 keV Mn Kα line and 1 μs shaping time, and 25 μm thick Be entrance window. A further absorber (450 μm Mylar foil) is mounted to attenuate the low energy X-rays. In the upgraded set-up, a second SDD, with the same characteristics as the previous one, has been introduced, with the same geometry, so that both of them are placed at 135° with respect to the beam direction, at a distance of about 2–2.5 cm from the target. This results in a doubled solid angle, and therefore in a doubled statistics of the acquired spectra (obtained as the sum of the two single spectra). As a whole, the SDD array of the upgraded set-up covers a total solid angle of 400 msr.

The performance of the upgraded set-up has been compared to that of the previous one in terms of detection efficiency by measuring by PIXE, in the same experimental conditions, a set of thin standards of known areal density supplied by Micromatter with the previous and the upgraded set-ups. The obtained sensitivity curves, expressed as counts/μC/(μg/cm^2) as a function of X-ray energy, are reported in Fig. 3: as can be clearly seen, with the new detecting systems an increase of the sensitivity by a factor about 2.5 has been obtained for the detection of both low-Z and medium-high-Z elements, thus maintaining the balance between their counting rates.

The introduction of the SDDs had already allowed the increase of the used beam currents up to 100–300 nA, swapping the limit from the sustainability of the counting rate by the detection system to the difficulty of obtaining higher currents with the LABEC accelerator system and also of managing them in terms of damage of the sample. Therefore, with the previous set-up, measuring times down to 30 s per 1-h sample were already possible, in case of rich aerosol deposits; however, longer measuring times had to be used in case of samplings performed in remote or suburban areas, or with low-pollution conditions, in order to get a good spectrum statistics. Nowadays, measuring times down to 30 s may be
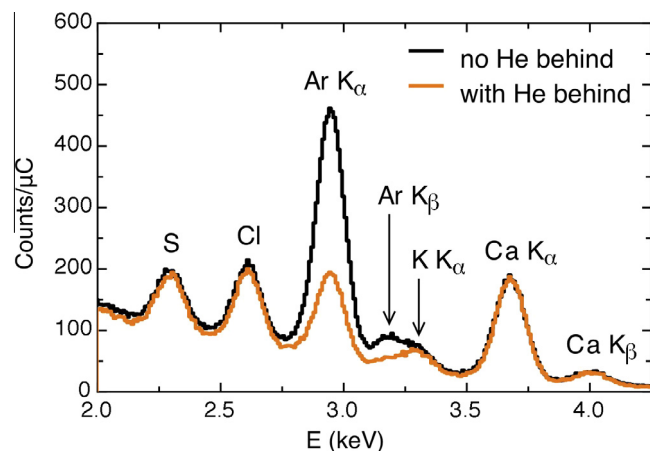

Fig. 1. Picture of the newly upgraded external beam PIXE set-up, with the SDD array, i.e., the 30 mm^2 SDD for low-Z element detection (upper part of the picture, showing also the magnetic proton deflector assembly) and the two 80 mm^2 SDDs for the detection of medium-high-Z elements (on the left and right); the Si_3N_4 extraction window is visible in the center of the figure.

Fig. 2. Comparison of PIXE spectra acquired with and without helium flow behind the target (i.e., between the target and the Faraday cup).
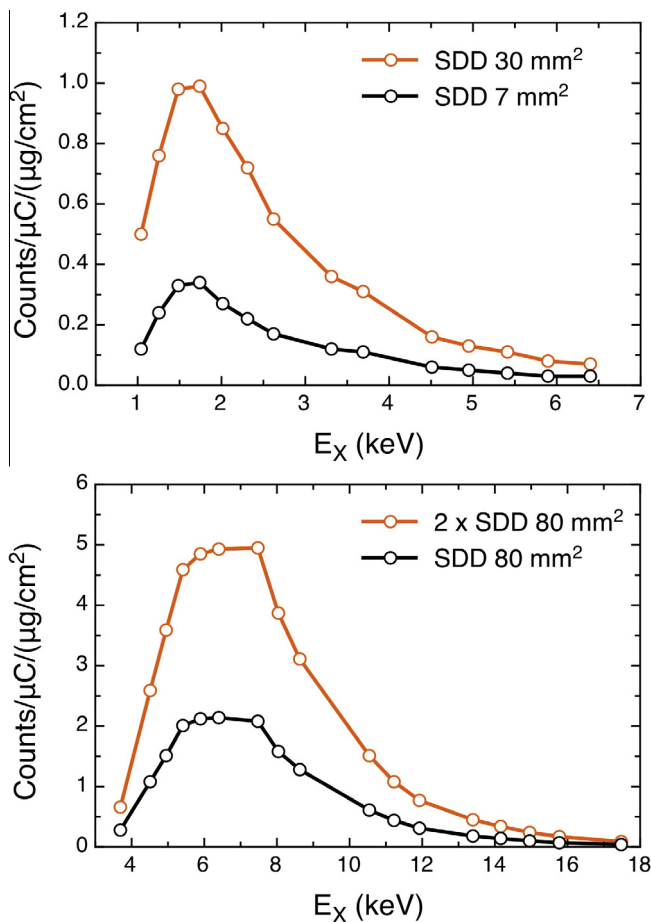
Fig. 3. Comparison of sensitivity curves as a function of X-ray energy for the previous and the new PIXE detection systems as concerns the low-Z elements (upper panel) and medium-high-Z elements (lower panel).

used for most of the samples, while longer times (e.g., 1 min) may be used to achieve better detection limits. It is worth noting that nowadays the measurement of a streaker foil or filter may take less than 2 h, with still better detection limits than the ones that were obtained when using the Si(Li) detectors and 9 h of measuring time. The reduction of the streaker measuring time, together with the high request of compositional data with hourly resolution for aerosol research studies, has led to a constant increase of the application of PIXE on streaker samples at LABEC, as shown in Fig. 4.

When dealing with the high-throughput and speed of the measurements, a comment on the beam extraction window is also mandatory: in the earlier times [21], a 7.5 μm thick Upilex-S ($C_{22}H_{10}N_2O_4$, density 1.47 g/cm^3) foil was used for such purpose, but it needed to be replaced every 2–3 h when extracting a 3 MeV proton beam of about 100 nA intensity, due to the progressive damage of the foil, resulting in its thinning and subsequent rupture. Since 2012, a 500 nm thick, 3×3 mm^2 large Si$_3$N$_4$ window supplied by Silson Ltd. is in use, with no need of any time-consuming replacements in about 3 years of use.

The analysis of streaker samples is performed measuring the deposit streak point-by-point, using a beam collimated in order to get a spot corresponding to 1-h sampling, i.e., 1×2 mm^2. The deposit on the filtration foil actually exceeds the beam spot dimensions, since during 1-h sampling the produced spot is around 1×7 mm^2: a continuous scanning is performed moving the sample up and down in order to average out possible deposit inhomogeneities caused by possible slight air flow inhomogeneities through the sucking orifice [18].
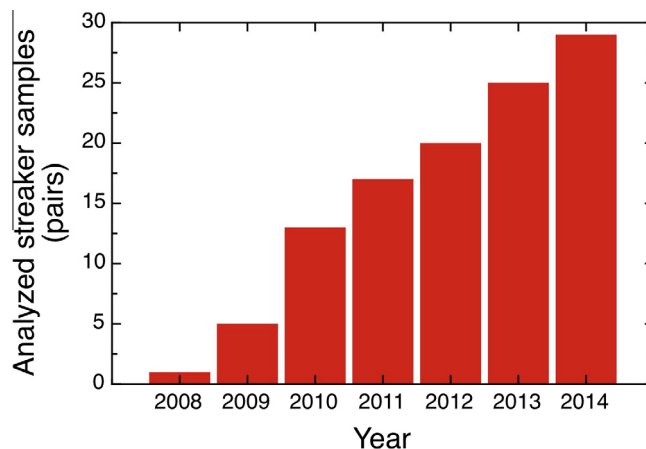

Fig. 4. Number of streaker samples (fine and coarse fraction pairs) analyzed per year at the LABEC laboratory.

3.2. Choice of the proton beam energy

As it is well known, the increase of the proton beam energy in PIXE measurements results in higher statistics of the X-ray lines due to the increase of the X-ray production cross sections, but also in an increase of the background beneath them. Therefore, with the aim of choosing the optimal beam energy to perform the measurements on the streaker samples, a systematic study of the minimum detection limits (MDLs) was performed as a function of the energy of the proton beam. PIXE measurements were performed on both streaker Kapton foil and Nuclepore filter at proton beam energies (on target) ranging from 2.0 to 3.5 MeV; in fact, for lower beam energies X-ray emission production sections are very low, while for higher energies nuclear reaction channels both in the sample or in the residual air (e.g., on nitrogen isotopes) can be opened, leading to the production of γ-rays that increase the Compton background in the spectra, with an overall worsening of the MDLs [24]. As can be seen in Fig. 5, for high-Z elements the effect of the increase of the X-ray production cross sections prevails, and the MDLs improve with the increase of the beam energy up to 3.0 MeV, remaining almost stable when it is further increased to 3.5 MeV due to the increase of the Compton background. On the other hand, low and medium-Z elements, whose X-rays are situated in a region of the spectrum with prominent bremsstrahlung background, suffer from the increase of the background more than they benefit from the increase of the cross sections: therefore, their MDLs worsen when increasing the beam energy from 2.0 to 3.5 MeV. Taking into account the importance of the high-Z elements in aerosol studies (they may be important markers of specific aerosol sources) and the average aerosol composition, with prevailing low-Z elements, proton beam energies between 2.5 and 3.0 MeV appear to provide the best compromise to measure all the detectable elements in aerosol samples.

3.3. Collection substrates

As previously mentioned, Nuclepore filters and Kapton foils are commercially available for the sampling with the streaker sampler; nevertheless, a research on alternative collecting substrates was carried out, looking for membranes/foils allowing lower background during the measurement, characterized by no or minimum contamination, and guaranteeing good performance during the sampling. On the basis of a literature and market research, some foils were selected and tested. In particular, as concerns the Nuclepore foil, no alternative filtering material was found with better
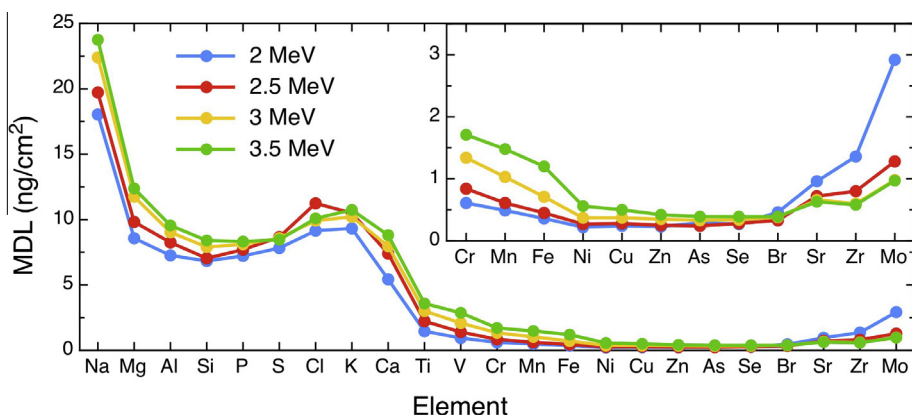
Fig. 5. Comparison of the MDLs for the various elements detectable by PIXE measurements on a Kapton streaker foil at proton beam energies ranging from 2.0 to 3.5 MeV. The MDLs for elements typically detected by the two 80 mm^2 SDDs are shown in detail in the inset.
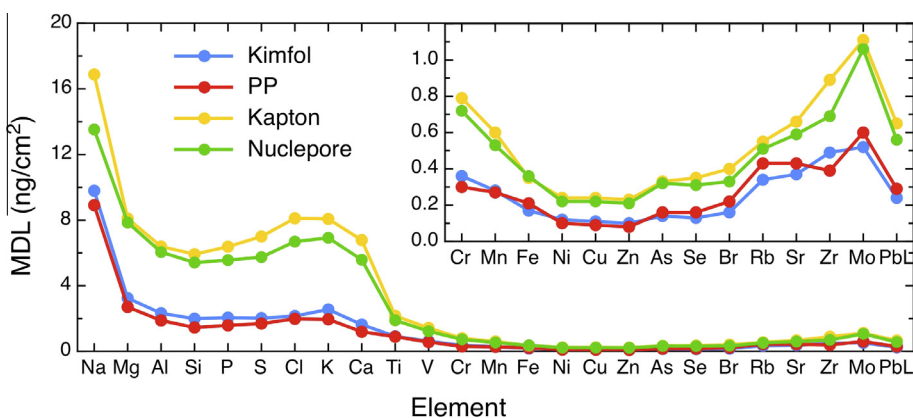

Fig. 6. Comparison of the MDLs for the various elements detectable by PIXE measurements with 2.5 MeV energy (on target) proton beam on different sampling substrates. The MDLs for elements typically detected by the two 80 mm^2 SDDs are shown in detail in the inset.

characteristics in terms of cleanliness, thickness and mechanical resistance. In fact, the most widespread alternative filtering materials are either much thicker (e.g., quartz fiber, mixed ester cellulose, unsupported Teflon filters) or unfitted to the large foil frames (about 10 cm of diameter) needed for the streaker cartridge. Therefore, tests were performed to choose the supplier providing the cleanest Nuclepore membranes.

On the other hand, as concerns the impaction stage, a material used in previous studies for cascade impactors [25], Kimfol, was tested as an alternative to the commercially available Kapton foils. First, the Kimfol was characterized by means of Elastic Back Scattering (EBS) and Particle Elastic Scattering Analysis (PESA) measurements performed with a 3.6 MeV proton beam in the in-vacuum set-up available at LABEC: Kimfol was found to have a composition according to the formula $C_{0.48}H_{0.44}O_{0.08}$ (thus similar to Nuclepore) and a $1.80 \pm 0.09\ \mu m$ thickness. Spectra acquired during PIXE measurements on blank Kimfol foils showed that they do not contain any contaminations visible with PIXE analysis, and that the bremsstrahlung background is much lower than in spectra acquired in the same experimental conditions on a blank Kapton foil, due to the fact that Kimfol is much thinner than Kapton. Therefore, Kimfol appeared to be a better substrate for streaker sampling. However, as it is currently out of stock and not produced anymore, although the LABEC laboratory has still a good availability of it, also other materials were considered. In particular, analogous tests were performed on Polypropylene (C_3H_6) foils, 4 μm thick, confirming their cleanliness and low background in the PIXE

spectra. All impaction foils were coated with a solution of Apiezon Grease L in Toluene to avoid the bouncing of particles, and tests were performed to check that no contamination was introduced with this step.

A comparison of the typical MDL achieved in real measurements on samples collected on the different substrates with a 2.5 MeV proton beam (energy on target) is reported in Fig. 6: thinner substrates (Kimfol and PP) clearly have better performance in terms of MDL, especially for the elements up to Ca, whose X-rays lay in a spectrum region with prominent bremsstrahlung background.

4. Conclusions

At the LABEC laboratory of INFN in Florence, where a 3 MV Tandetron accelerator is available, the external beam set-up fully dedicated to PIXE analysis of aerosol samples has been upgraded introducing two new SDD detectors; one of them replaces a similar detector with smaller active area and is dedicated to the detection of low-Z elements, the second one pairs with another SDD with the same characteristics, already available in the set-up, with the result of doubling the solid angle and therefore the statistics for the detection of medium-high-Z elements. Furthermore, the choice of an optimal proton beam energy for the measurements (2.5 MeV on target) and of suitable collecting substrates has allowed better detection limits for PIXE analysis of streaker samples. With these

improvements, the LABEC laboratory has enhanced its capability in high-throughput and high-sensitivity analysis of aerosol samples, and especially of PM samples collected with hourly resolution, in particular with the streaker sampler. This, together with the high request of compositional data with hourly resolution for aerosol research studies, has strongly risen the application of PIXE on streaker samples at LABEC. This result confirms that, despite the number of competitive techniques, PIXE still holds an outstanding position in atmospheric aerosol research, provided that its potential is fully exploited using a proper experimental set-up and optimized measurement parameters.

Acknowledgments

References

[1] C.A. Pope, D.W. Dockery, J. Air Waste Manage. Assoc. 56 (2006) 709.
[2] O. Boucher, D. Randall, P. Artaxo, C. Bretherton, G. Feingold, P. Forster, V.-M. Kerminen, Y. Kondo, H. Liao, U. Lohmann, P. Rasch, S.K. Satheesh, S. Sherwood, B. Stevens, X.Y. Zhang, Clouds and aerosols, in: T.F. Stocker, D. Qin, G.-K. Plattner, M. Tignor, S.K. Allen, J. Boschung, A. Nauels, Y. Xia, V. Bex, P.M. Midgley (Eds.), Climate Change 2013: The Physical Science Basis. Contribution of Working Group I to the Fifth Assessment Report of the Intergovernmental Panel on Climate Change, Cambridge University Press, Cambridge, United Kingdom and New York, NY, USA, 2013.
[3] V.A. Marple, K. Willeke, Atmos. Environ. 10 (1976) 891.
[4] V. Bernardoni, G. Calzolai, M. Chiari, M. Fedi, F. Lucarelli, S. Nava, A. Piazzalunga, F. Riccobono, F. Taccetti, G. Valli, R. Vecchi, J. Aerosol Sci. 56 (2013) 88.
[5] M. Viana, T.A.J. Kuhlbusch, X. Querol, A. Alastuey, R.M. Harrison, P.K. Hopke, W. Winiwarter, M. Vallius, S. Szidat, A.S.H. Prévôt, C. Hueglin, H. Bloemen, P. Wåhlin, R. Vecchi, A.I. Miranda, A. Kasper-Giebl, W. Maenhaut, R. Hitzenberger, J. Aerosol Sci. 39 (2008) 827.
[6] M. Chiari, F. Lucarelli, A. Migliori, S. Nava, G. Valli, R. Vecchi, I. Garcia-Orellana, F. Mazzei, Nucl. Instr. Meth. B 249 (2006) 552.
[7] M. Chiari, P. Del Carmine, I. Garcia Orellana, F. Lucarelli, S. Nava, L. Paperetti, Nucl. Instr. Meth. B 249 (2006) 584.
[8] F. Amato, M. Viana, A. Richard, M. Furger, A.S.H. Prevot, S. Nava, F. Lucarelli, N. Bukowiecki, A. Alastuey, C. Reche, T. Moreno, M. Pandolfi, J. Pey, X. Querol, Atmos. Chem. Phys. 11 (2011) 2917.
[9] J. Crespo, E. Yubero, J.F. Nicolás, F. Lucarelli, S. Nava, M. Chiari, G. Calzolai, J. Hazard. Mater. 241–242 (2012) 82.
[10] T. Moreno, A. Karanasiou, F. Amato, F. Lucarelli, S. Nava, G. Calzolai, M. Chiari, E. Coz, B. Artíñanod, J. Lumbreras, R. Borge, E. Boldo, C. Linaresf, A. Alastuey, X. Querol, W. Gibbons, Atmos. Environ. 68 (2013) 33.
[11] T. Moreno, T. Kojima, F. Amato, F. Lucarelli, J. de la Rosa, G. Calzolai, S. Nava, M. Chiari, A. Alastuey, X. Querol, W. Gibbons, Atmos. Chem. Phys. 13 (2013) 1411.
[12] M. Dall'Osto, X. Querol, F. Amato, A. Karanasiou, F. Lucarelli, S. Nava, G. Calzolai, M. Chiari, Atmos. Chem. Phys. 13 (2013) 4375.
[13] M. Viana, C. Reche, F. Amato, A. Alastuey, X. Querol, T. Moreno, F. Lucarelli, S. Nava, G. Calzolai, M. Chiari, M. Rico, Atmos. Environ. 72 (2013) 81.
[14] A.M. Taiwo, D.C.S. Beddows, G. Calzolai, R.M. Harrison, F. Lucarelli, S. Nava, Z. Shi, G. Valli, R. Vecchi, Sci. Total Environ. 490 (2014) 488.
[15] S. Nava, F. Lucarelli, F. Amato, S. Becagli, G. Calzolai, M. Chiari, M. Giannoni, R. Traversi, R. Udisti, Sci. Total Environ. 511 (2015) 11.
[16] F. Lucarelli, S. Nava, G. Calzolai, M. Chiari, R. Udisti, F. Marino, X-ray Spectrom. 40 (2011) 162.
[17] M. Giannoni, G. Calzolai, M. Chiari, F. Lucarelli, A. Mazzinghi, S. Nava, C. Ruberto, X-ray Spectrom. 44 (2015) 282.
[18] PIXE International Streaker, <http://www.pixeintl.com/Streaker.asp>.
[19] P. Del Carmine, L. Giuntini, W. Hooper, F. Lucarelli, P.A. Mandò, Nucl. Instr. Meth. B 113 (1996) 354.
[20] M. Chiari, F. Lucarelli, F. Mazzei, S. Nava, L. Paperetti, P. Prati, G. Valli, R. Vecchi, X-ray Spectrom. 34 (2005) 323.
[21] G. Calzolai, M. Chiari, I. García-Orellana, F. Lucarelli, A. Migliori, S. Nava, F. Taccetti, Nucl. Instr. Meth. B 249 (2006) 928.
[22] F. Lucarelli, G. Calzolai, M. Chiari, M. Giannoni, D. Mochi, S. Nava, L. Carraresi, Nucl. Instr. Meth. B 318 (2014) 55.
[23] T. Eggert, P. Goldstrass, J. Kemmer, A. Pahlke, Nucl. Instr. Meth. A 512 (2003) 257.
[24] G. Calzolai, M. Chiari, F. Lucarelli, S. Nava, S. Portarena, Nucl. Instr. Meth. B 268 (2010) 1540.
[25] W. Maenhaut, R. Hillamo, T. Mäkelä, J.-L. Jaffrezo, M.H. Bergin, C.I. Davidson, Nucl. Instr. Meth. B 109 (110) (1996) 482.